mathematics

MDPI

Article

Investigating the Influence of Non-Uniform Characteristics of Layered Foundation on Ground Vibration Using an Efficient 2.5D Random Finite Element Method

Shaofeng Yao [1,2], Liang Yue [3], Wei Xie [4], Sen Zheng [5], Shuo Tang [6], Jinglong Liu [6] and Wenkai Wang [3,*]

1 College of Civil Engineering and Architecture, Zhejiang University of Water Resources and Electric Power, Hangzhou 310000, China; yaoshf@zjweu.edu.cn
2 Department of Geotechnical Engineering, Tongji University, Shanghai 200092, China
3 China Waterborne Transport Research Institute, Beijing 100088, China; yueliang@wti.ac.cn
4 Powerchina Huadong Engineering Co., Ltd., Hangzhou 310000, China; xie_w2@hdec.com
5 ENAC/IIC/LHE, Ecole Polytechnique Fédérale de Lausanne, CH 1015 Lausanne, Switzerland; sen.zheng@epfl.ch
6 Tianjin Branch, CNOOC (China) Co., Ltd., Tianjin 300457, China; tangshuo@cnooc.com.cn (S.T.); liujl15@cnooc.com.cn (J.L.)
* Correspondence: wangwenkai@wti.ac.cn

Abstract: High-speed train operation may cause vibration near track facilities and propagate far through the ground, affecting people's lives, work, and normal use of precision instruments in an urban environment. An efficient numerical method is proposed to calculate the non-uniform ground vibration under a moving high-speed railway load. The theory of stochastic variables is used to describe the soil spatial variability of the non-uniform layered elastic ground, and the coupled 2.5D random finite element method (FEM) is proposed to reduce the computational cost without losing accuracy. Vibration propagation and attenuation of the non-uniform layered ground are investigated and the effect of train speed and soil non-homogeneity are analyzed. Results show that (1) at cross speed and high speed, the homogeneity coefficient of the layered ground has the most important influence on the ground vibration amplitude; (2) the upward acceleration is much larger than the downward acceleration at most speeds, and at cross speed and high speed, the acceleration amplitude decreases with the increase in the homogeneity coefficient; (3) as train speed increases from 60 m/s to 130 m/s, the influencing range of the homogeneity coefficient increases to 10 m from 2 m; and (4) the phenomenon of an in increase in local rebound can be observed in the velocity and acceleration attenuation curve at cross speed when the ground soil has a weaker homogeneity.

Keywords: numerical simulation; high-speed railway; soil non-homogeneity; ground vibration; 2.5D random FEM

MSC: 74-10; 74H45; 74B05; 75G15; 65N30; 65P99

Citation: Yao, S.; Yue, L.; Xie, W.; Zheng, S.; Tang, S.; Liu, J.; Wang, W. Investigating the Influence of Non-Uniform Characteristics of Layered Foundation on Ground Vibration Using an Efficient 2.5D Random Finite Element Method. *Mathematics* **2024**, *12*, 1488. https://doi.org/10.3390/math12101488

Academic Editor: Huaizhong Zhao

Received: 17 April 2024
Revised: 5 May 2024
Accepted: 7 May 2024
Published: 10 May 2024

1. Introduction

In recent years, high-speed railway (HSR) has developed as a convenient means of transportation in China. The HSR operation may cause vibration near track facilities and propagate far through the ground, affecting people's lives, work, and normal use of precision instruments in an urban environment [1]. Hence, it has become a key challenge to reasonably evaluate the ground vibration caused by trains and its impact on the adjacent environment in HSR construction.

Investigations concerning the ground vibration induced by moving surface loads date back to the 1950s, and have been reviewed in detailed by Beskou and Theodorakopoulos [2], from track–ground models to computation methods of the dynamic system. Researchers have allocated many efforts to this subject using analytical [3,4], numerical (such as FEM

and BEM) [5,6], or semi-analytical methods [7,8]. The moving loads may cause the Doppler or Mach radiation effects of a traveling wave at some critical speed, due to the properties of wave propagation in the embankment–ground system and the bending wave propagation in the track [2,6]; these can be simulated through the 3D FEM model, but this is usually too time-consuming in practice. An accurate 3D numerical model often has a large computational cost due to the high speed of HSR (250–400 km/h), while a simplified 2D plane strain numerical model often lowers the result precision although it has a higher calculation speed. In order to avoid the shortcomings of 2D/3D numerical models and fully utilize their advantages, Yang and Hung [9,10] proposed a two-and-a-half finite element method (2.5D FEM) to study the ground dynamic response under moving train loads. The same numerical concept was also adopted by Takemiya and Bian [11–13] to evaluate the dynamic stress and long-term settlement of the layered ground under a moving railway load. In this semi-numerical model, the geometric shape and material properties of the track structure–elastic soil are assumed to be unchanged along the moving load, and the finite element discretization in the numerical calculation is only required in the section perpendicular to the track; hence, the 2.5D FEM can significantly reduce the numerical computational cost by about 200 times without losing accuracy [10,14,15].

As suggested by Dieterman et al. [7] and Sheng et al. [16], the elaborated physical soil characteristic should be described as close to the actual situations as possible, since it has an important effect on the numerical accuracy of the track–ground dynamic response. In most of the previous studies, the granular soil medium is usually treated as a homogeneous material, and the effect of soil spatial variability on the ground vibration is often neglected. In fact, it is well known that the soil properties are inherently variable and have considerable randomness, which leads to strong non-uniformity even within "homogeneous" ground layers [17,18] and often makes deterministic predictions of vibration propagation inaccurate [19]. Analyses of the impacts of soil variability on the ground seismic/dynamic response have been conducted using stochastic field theory [20–23]. As another method to consider the soil non-uniform characteristics, stochastic variable theory is also widely used due to its simplicity, small computational cost, and high efficiency [24,25]. Assimki et al. [24] investigated the influence of soil space change on ground movement using the standard Monte Carlo (MC) simulation framework, and found that changes in soil properties have a considerable impact on ground vibration. To investigate the spatial heterogeneity of soil stiffness on wave propagation, Coelho et al. [26] developed a dynamic random finite element model by means of random variable theory and the Monte Carlo approach. To obtain reliable vibration and attenuation prediction, spatial variability should be undoubtedly included in the simulation of train-induced ground vibration. In previous studies, uniform elastic or layered ground vibrations under railway loads have attracted a large amount of attention [9–16,27–29]. However, until now, only a few works concerning non-uniform soil have been undertaken to elucidate the impact of soil non-homogeneity on the ground vibration and propagation. For example, Gao et al. [30] established a semi-analytical boundary element method based on the thin-layer method to analyze the 3D non-uniform ground vibration caused by a train load, pointing out that the non-uniform coefficient has an important impact on the vibration isolation. Zhou et al. [31] employed integral transformation and elastic dynamic theory to analyze the vibration characteristics of a 2D non-uniform foundation having a shear modulus that linearly varied with depth, and results showed that the load speed and soil non-uniformity significantly affected the dynamic response of the foundation. Ma et al. [32] established the governing equation for the dynamic response of gradient non-uniform soil under a moving load and analyzed the influence of soil non-uniformity using the back propagation ray matrix method. Although not commonly used, other methods, such as the finite difference method and differential quadrature method [33–35], are also useful for the further study of the ground vibration caused by train loads. It is shown in these studies that the non-uniform characteristics of ground soil is of great significance and worth considering to understand the special characteristics and propagation of the ground vibration.

In this study, an efficient numerical method is established to investigate the vibration of non-uniform layered ground under an HSR load, with consideration of the soil spatial variability. The theory of stochastic variables is adopted to describe the non-uniform layered elastic ground, and a semi-numerical 2.5D random FEM program is proposed to solve the coupled model. The 3D problems then can be solved using the 2D plane numerical model, and the results can be quickly and accurately derived in a single computation, which can significantly reduce the computation cost without losing accuracy. Finally, ground vibration and attenuation characteristics of a layered elastic foundation considering the spatial variability of surface soil are investigated, and numerical calculations at different train speeds are conducted to analyze the influence of train speed and soil non-homogeneity on the ground vibration.

2. Analysis Model and Solution Method

2.1. Formulation of 2.5D FEM Considering Spatial Variability

2.1.1. Basic 2.5D Finite Element Model

In elasto-dynamic theory, the governing equation is actually a partial differential equation system [5,6]. When we perform Fourier transform on the time term and load moving direction variables of the dynamic equations, the final formulation for the 2.5D finite element numerical method of an elastic medium can be derived and expressed as follows [9,10]:

$$(K - \omega^2 M) \times \overline{\overline{u}} = F \tag{1}$$

where ω is the circular frequency, $\overline{\overline{u}}$ and F are the node displacement of the ground soil and external equivalent node load in the frequency–wavenumber domain, and K and M are the coefficient matrices of stiffness and mass, expressed as follows:

$$F = \sum_e N^T f |J| d\eta d\varepsilon$$

$$M = \sum_e \rho^e \iint N^T N |J| d\eta d\varepsilon$$

$$K = \sum_e (B^* N)^T D (BN) |J| d\eta d\varepsilon$$

in which D is the stress matrix and B is the partial derivative matrix of the elastic medium; the superscript '*' and 'T' represent the conjugate and transpose of the matrix; J is the Jacobi matrix; f is the equivalent node load vector; and N is the shape function of a 4-node isoparametric finite element for discretization, and can be expressed as:

$$N_i(\eta, \xi) = \frac{1}{4}(1 + \eta_i \eta)(1 + \xi_i \xi)$$

where η, ξ are local coordinates of the element and η_i, ξ_i are node coefficients. Readers can refer to more details in the study presented by Yang and Hung [9,10] about the derivation process and parameter meanings.

2.1.2. Consideration of the Soil Spatial Variability

In non-uniform ground soil, the interior of the soil elements is considered to be uniform, while each element is distributed independently with a randomized physical property. The physical property (e.g., elastic modulus) of each element varies with its spatial position and has a Weibull statistical distribution [36,37], and the probability distribution function is as follows:

$$f(x, \lambda, \beta) = \begin{cases} \frac{\beta}{\lambda}(\frac{x}{\lambda})^{\beta-1} \exp(-(\frac{x}{\lambda})^{\beta}) & x \geq 0 \\ 0 & x < 0 \end{cases} \tag{2}$$

where x and λ represent the unit mechanic parameters and its average level in the soil layer, and β represents the shape parameter of the distribution function, which is called the homogeneity coefficient of the soil medium. This distribution function was adopted by Lei [37] to simulate the spatial heterogeneity and spatial distribution law of the soil's physical and mechanical parameters, which provided distinct advantages over traditional models in simplicity and efficiency. This relationship is then directly incorporated into the 2.5D FEM model presented in the previous part to consider the influence of the soil spatial variability. As shown in Figure 1, the probability distribution function is strongly influenced by the shape parameter β. By changing the shape parameter of the model, the influence of the non-uniformity of the soil on the ground vibration can be considered. It can be observed that when there is a smaller homogeneity coefficient (e.g., taken as 2), the distribution range of the soil element property parameter has a wide scope, indicating a weaker homogeneity of the ground soil. In the most common scenario, the median value of 5 is taken, and is used here. At a specific homogeneity coefficient value, sufficient automatic Monte Carlo simulations (MCs) were conducted on the computers to generate random variables with a convergent mean value of the probability characteristic. The physical property values with a non-uniform distribution for the soil cells serve as the calculation parameters in the finite element calculation at each specific uniform coefficient.

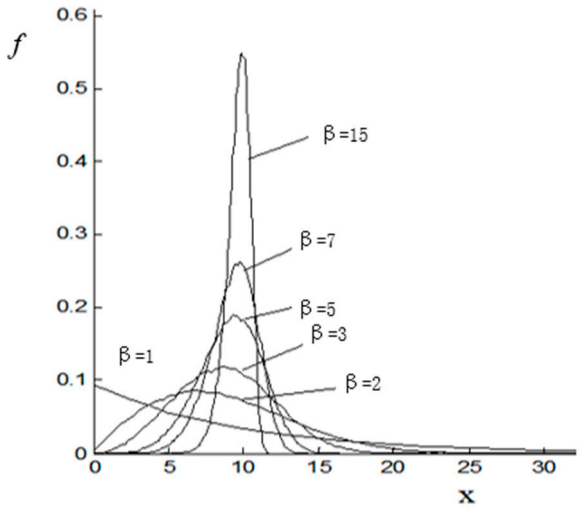

Figure 1. Probability distribution function of the Weibull statistical distribution influenced by the shape parameter.

2.1.3. Track System Modeling and Train Loads

In the research on ground vibration, it is generally believed that the entire track system undergoes an overall deformation under train loads. The track system (including the rails and the embankment) can be simulated as a composite Euler beam with a bending stiffness of EI [12,14], and the dynamic equation of the track structure in the frequency–wavenumber domain under load $p_0\delta(x - ct)$ can be expressed as [12]:

$$(EI\xi_x^4 - m\omega^4)u_r^{xt} = f_{IT}^{xt}(\xi_x, \omega) + p_0^{xt}(\xi_x, \omega)$$

and expressed in a matrix form as:

$$K_{TT}U_{TT} = F_{IT} + F_T \tag{3}$$

where ξ_x is the wave number variable, m is the comprehensive mass of the track system, u_r^{xt} is the displacement of the track in the frequency–wavenumber domain, and $p_0^{xt}(\xi_x, \omega)$ and $f_{IT}^{xt}(\xi_x, \omega)$ are the external dynamic train load on the track and the reactive force at the foundation contact point in the frequency–wavenumber domain, respectively. U_{TT} represents three orthogonal displacement vectors of the track nodes (including vertical

displacement and two horizontal displacements). The coupled elastic 2.5D random FEM calculation model for the track non-uniform ground under a high-speed railway load can be obtained by combining Equations (1)–(3).

Consider a train comprising N cars, where each car has four pairs of wheels and the train load acts on the track moving along the x-direction with a velocity of V_c. Based on the geometry and loading information of the train [12], the series of train wheel loads in the frequency–wavenumber domain is directly described mathematically as follows:

$$\widetilde{\overline{p}}(\xi_x, y, z, \omega) = \frac{2\pi}{V_c}\delta(\xi_x - \frac{\omega}{V_c})\chi(\xi_x)$$

where $\chi(\xi_x) = \sum_{n=1}^{N-1}[P_{n1}(1 + exp(-ia_n\xi_x) + P_{n2}(exp(-i(a_n + b_n)\xi_x) + exp(-i(2a_n + b_n)\xi_x)]$ $exp(-i\sum_{k=0}^{N-1} L_k\xi_x)$, P_{n1} and P_{n2} are the axle loads for the front and rear bogies; L_0 is the distance to a reference position ahead of the first axle load position and L_i is the ith car length; a_n, b_n are the distances between axles.

Figure 2 shows the schematic diagram of the coupled track non-uniform layered ground model established in this paper. The vertical cross-section of the track–soil is discretized using 4-node isoparametric elements, and visco-elastic wave absorbing boundaries truncate the modeling space at both sides to prevent the reflection of the external traveling waves [38]. During programming, the train load in the frequency–wavenumber domain is directly applied to the contact points between the track and foundation model. An iterative calculation is performed to solve the governing equations and the double Fourier transform is conducted to obtain the dynamic response in the time–space domain, and this can be simplified to a single Fourier transform using the property of the Dirac function to improve efficiency.

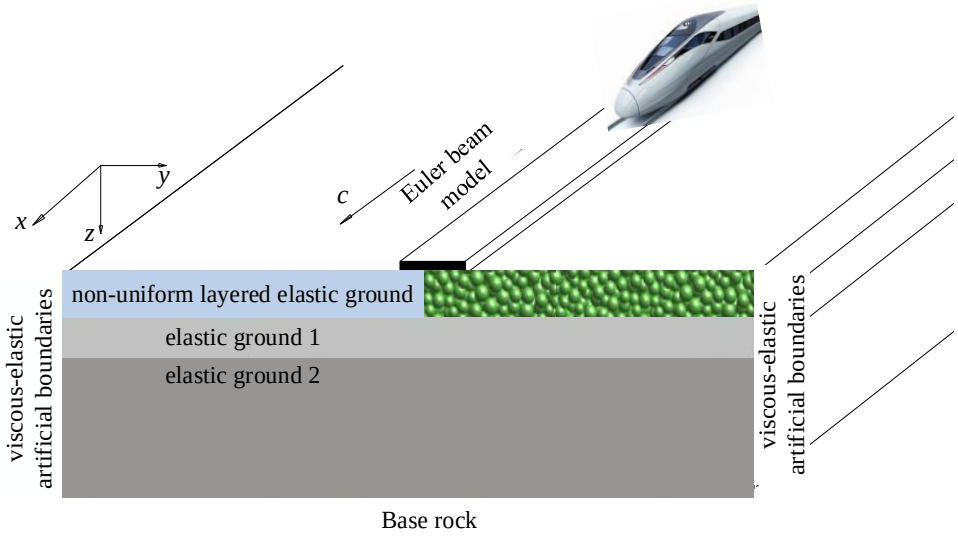

Figure 2. Schematic diagram of the coupled track non-uniform layered elastic ground.

2.2. Program Verification of the Coupled 2.5D Random FEM

In this section, the verification of the coupled 2.5D random FEM for an elastic medium is carried out in two steps. Firstly, the existing analytical solution for a 3D homogeneous half-space subjected to a moving load is compared with the results of the 2.5D FEM program used in this study. Subsequently, we degenerate the coupled non-uniform elastic 2.5D random FEM model to the uniform model and compare the result with the existing analytical solution for elastic media.

2.2.1. Verification of 2.5D FEM Calculation Program

The analytical solution [3] is used for comparison and verification. Here, the ground of a half-space is approximated by a 20 m × 20 m uniform soil layer on a rigid rock layer, and a vertical point load is applied to the ground surface with a velocity of 90 m/s in the *x*-direction. Visco-elastic boundaries are used on both sides of the model, and a fixed boundary is used at the bottom. The density, elastic modulus, Poisson's ratio, and shear-wave velocity of the soil are 2000 kg/m^3, 50 MPa, 0.25, and 100 m/s, respectively, and the material damping coefficient is 0.05. The mesh size of the element is 0.5 m × 0.5 m, and there are 40 elements in both directions, as shown in Figure 3. The nodes and elements are numbered in an *S*-shaped pattern from the top left to the bottom right. The degrees of freedom for bottom fixed nodes are marked as 0, and the unknown degrees of freedom are marked as 1 in the programming process. There are 41 fixed constraints at the bottom nodes. The load is applied to the node marked 821 in the vertical direction. The dynamic response of the node marked 823 located 1.0 m beneath the surface load is investigated. The normalized horizontal and vertical displacement multiplied by $2\pi\rho V_s^2/P$ is presented in Figure 4. The analytical solution [3] is also depicted for comparison, and the two solutions are in good agreement, indicating the reliability of the 2.5D FEM program in this paper.

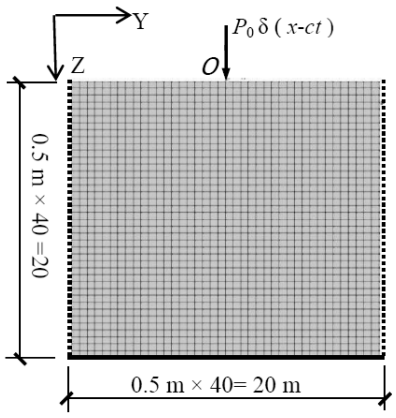

Figure 3. Element mesh of the ground section subjected to a vertical point load.

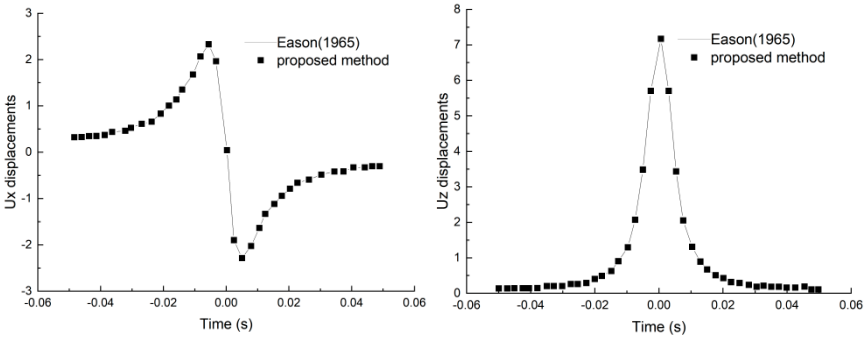

Figure 4. Verification of the 2.5D FEM model for elastic soil at 90 m/s [3].

2.2.2. Verification of Non-Uniform Elastic Soil Model

The coupled 2.5D random FEM model for the non-uniform elastic soil degenerates into the uniform model when the shape parameter takes a sufficiently large value (here taken as 200). In this situation, we can inspect the displacement results in three directions, as shown in Figure 5, where the subscript "z" represents the vertical direction, "x" represents the moving load direction, and "y" represents the lateral direction perpendicular to the moving load. The results of the coupled 2.5D random FEM model are in good agreement with the analytical solution [3] when degenerated to the uniform model, illustrating the reliability of the present model. Furthermore, it can be observed that the lateral displacement is almost zero and the displacement in the moving load direction is small enough to be ignored

compared to the vertical displacement; therefore, only vertical displacement is considered in the analysis hereafter.

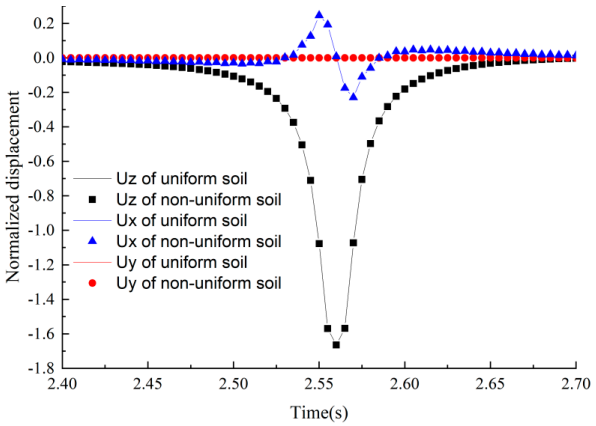

Figure 5. Normalized displacement in three directions as non-uniform soil degenerates into uniform soil.

3. Analysis of the Key Factors Influencing the Ground Vibration

To clarify the key factors influencing the ground dynamic response and the choice of non-uniform parameters, the basic 2.5D FEM model proposed in Section 2.1.1 is used to study the vertical and horizontal ground displacement and its attenuation. The monitoring points are located with a spacing of 0.5 m on the ground surface. The benchmark values and variation range of the soil physical parameters, i.e., Young's modulus, Poisson's ratio, density, and load velocity, are listed in Table 1. The parameters remain at their benchmark values unless otherwise specified. The shear wave and Rayleigh wave velocity corresponding to the benchmark soil parameters are 114 m/s and 124 m/s, respectively. Table 2 shows the detailed values of the calculation parameters. Figure 6 shows the attenuation and decay rate of the maximum normalized ground displacement in the x and z- directions. It can be seen that the Z-direction displacement is much greater and also decays faster with distance than that of the X-direction within 4 m from the loading point. Figure 7 shows the attenuation of the normalized ground displacement when soil parameters and velocity vary according to Table 2. It can be clearly seen that Young's modulus and load velocity have enormous implications compared to Poisson's ratio and density. To quantitatively illustrate the sensitivity level of parameters affecting the vibration propagation, the concept of sensitivity in system analysis is introduced using a non-repetitive variance quantification. Here, sensitivity is defined as the sensitivity coefficient multiplied by the change rate of the input variable:

$$\eta_{ss} = \eta_{sr} \times \frac{\max x_r - \min x_r}{x}$$

Two sets of experimental parameters are taken at low and high levels, respectively, at moving point loads, and response data are normalized by the result at the loading point. The parameter sensitivity of normalized ground displacement is depicted in Figure 8. It can be found that the elastic modulus and train speed greatly affect the propagation and attenuation of ground vibration. Therefore, the influence of elastic modulus variability at different train speeds is investigated hereafter, and Poisson's ratio and density are considered deterministic.

Table 1. Basic parameters for ground vibration simulation in half-space.

Parameters	Young's Modulus (MPa)	Poisson's Ratio	Density (kg/m^3)	Load Velocity (m/s)
Benchmark Values	80	0.30	2000	70.0
Variation range	[20, 160]	[0.20, 0.45]	[1300, 2300]	[55.6, 164.0]

Table 2. Detailed values of calculation parameters for ground vibration simulation.

Young's Modulus (MPa)	Poisson's Ratio	Density (kg/m^3)	Load Velocity (m/s)
20	0.20	1300	55.6
25	0.23	1500	70.0
40	0.25	1700	83.3
60	0.30	1900	97.2
80	0.35	2100	111.1
100	0.40	2300	125.0
120	0.45	-	164.0
160	-	-	-

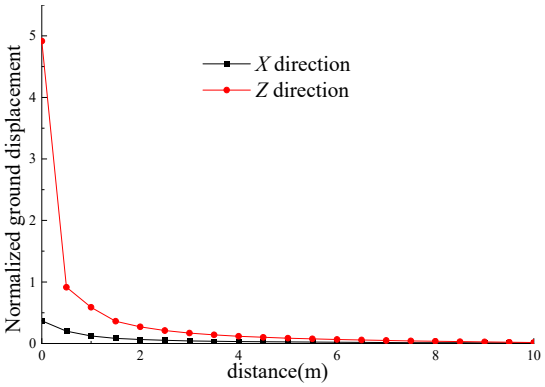

Figure 6. Normalized amplitude attenuation and decay rate of ground displacement in x and z directions with distance (U_{gt} = ground displacement amplitude at track center).

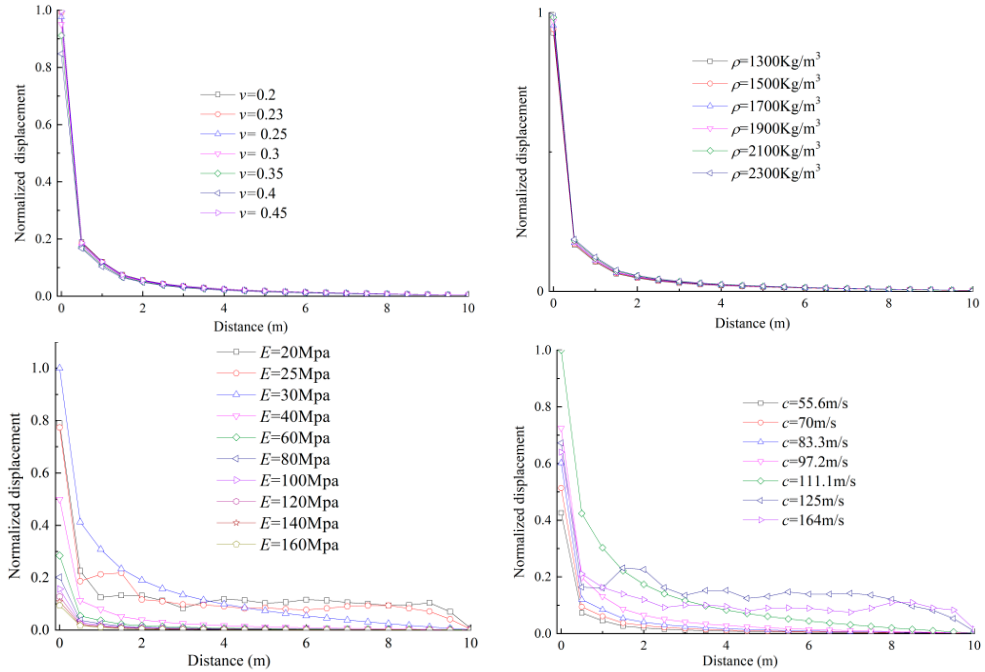

Figure 7. The attenuation of the normalized ground displacement with soil parameters and velocity.

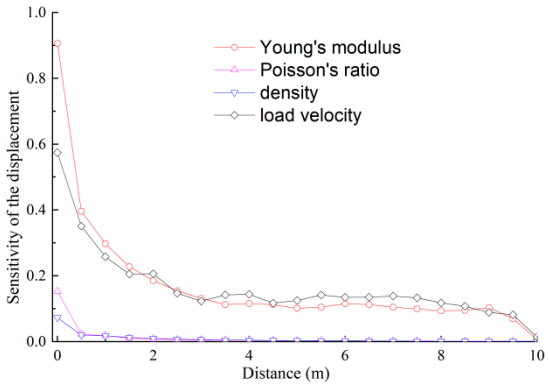

Figure 8. Parameter sensitivity analysis of the normalized maximum vertical displacement.

4. Vibration of Non-Uniform Elastic Layered Ground at Different Train Speeds

The calculation parameters for the non-uniform stratified ground are represented in Table 3, with 15, 5, and 2 chosen as representative coefficients to indicate the homogeneity of the soil elastic modulus. In practical geotechnical engineering, for soil with ordinary and better homogeneity, the coefficient can be 2–5, and if the soil homogeneity is excellent after soil improvement, the coefficient can be increased to 15–30. Regarding the train velocity, it is always paid special attention by researchers. Here, we choose typical speeds to consider their effect on the ground vibration. Costa et al. [39] pointed out that the critical speed of the stratified ground with an upper soft and lower hard soil layer is between the Rayleigh wave and shear wave velocity of the surface soil. This critical speed may cause resonance between the foundation soil and the moving train, which threatens the operational safety of the HRT. In the present study, the Rayleigh wave and shear wave velocity of the surface soil are 88.75 m/s and 95 m/s; therefore, 94.5 m/s is referred to as the "cross-speed" [40], which is faster than the Rayleigh wave speed and slower than the shear wave speed. Here, we also take 60 m/s as the low speed and 130 m/s as the high speed, and we numerically investigate the influence of the non-uniform characteristics of the layered foundation on ground vibration at these three train speeds.

Table 3. Calculation parameters of non-uniform stratified elastic ground.

Soil Layer No.	Thickness (m)	Shear Wave Velocity (m/s)	Density (kg/m^3)	Poisson's Ratio	Damping Coefficient	Mean Value of Elastic Modulus (10^7 pa)	Homogeneity Coefficient	Shear Modulus (10^7 pa)
1	2	95	1500	0.35	0.05	3.66	2, 5, 15	1.35
2	2	150	1700	0.30	0.05	9.95	200	3.83
3	26	280	1800	0.25	0.05	35.28	200	14.11

Figures 9–11 show the vertical acceleration time history curve of the ground surface at the track center under different ground homogeneity coefficients, and the train speeds are 60 m/s, 94.5 m/s, and 130 m/s respectively. We list different time history curves in the same vertical coordinate range, which helps readers to observe the amplitude changes with the homogeneity coefficient changes at the same vehicle speed. It can be seen that, at the same train speed, the shape of the acceleration curve remains almost unchanged at different values of β, and the acceleration upward is much larger than that downward at most speeds. At the same β, the acceleration increment is not obvious when the train speed increases from 94.5 m/s to 130 m/s. The ground acceleration exhibits a significant quasi-static effect of the wheel axle at 60 m/s, and displays a fluctuation in vibration acceleration at the high speed of 130 m/s. The non-homogeneity of the superficial soil affects the peak ground acceleration in a different way: at the low speed of 60 m/s (Figure 9), both upward and downward peak acceleration decrease significantly as β increases from 2 to 5. However, as β increases from 5 to 15, the peak acceleration change is not significant;

the upward peak acceleration is much larger than that of downward acceleration. At the cross speed of 94.5 m/s (Figure 10), the downward peak acceleration becomes as large as the upward acceleration at β = 2, and both upward and downward peak acceleration decrease as β increases from 2 to 15. When exceeding the cross speed and at the high-speed of 130 m/s (Figure 11), the upward peak acceleration continues to decrease as β increases from 2 to 15, while the downward peak value slightly increases, and the downward peak acceleration becomes as large as the upward acceleration at β = 15. It can be concluded that the non-uniformity of the superficial soil has a certain influence on the ground acceleration at the track center, especially for the cross speed and high speed.

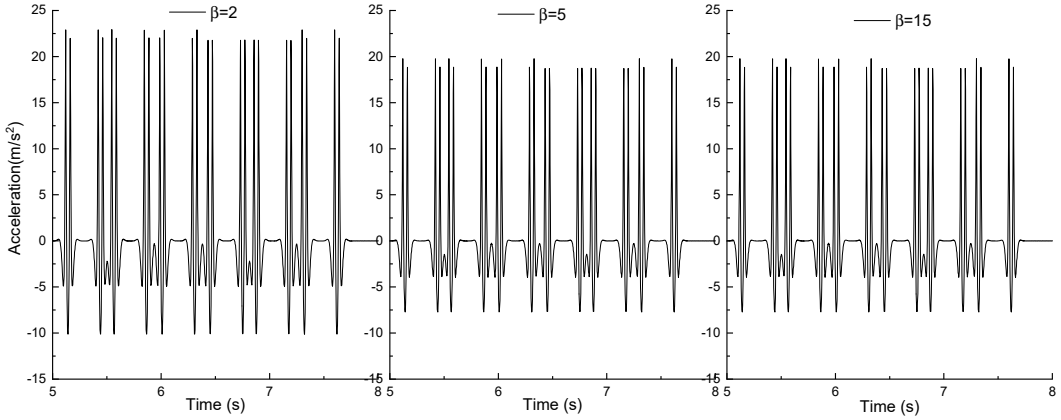

Figure 9. Time history curve of ground acceleration at the track center at 60 m/s.

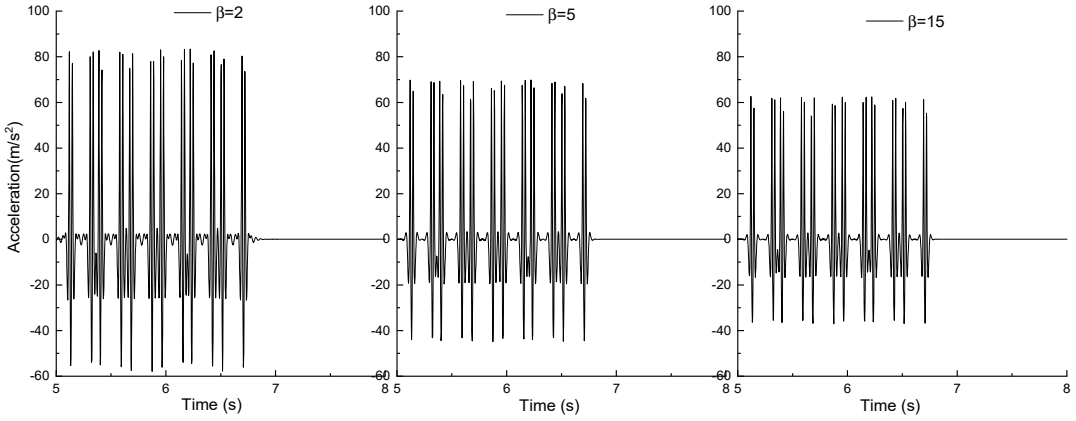

Figure 10. Time history curve of ground acceleration at the track center at 94.5 m/s.

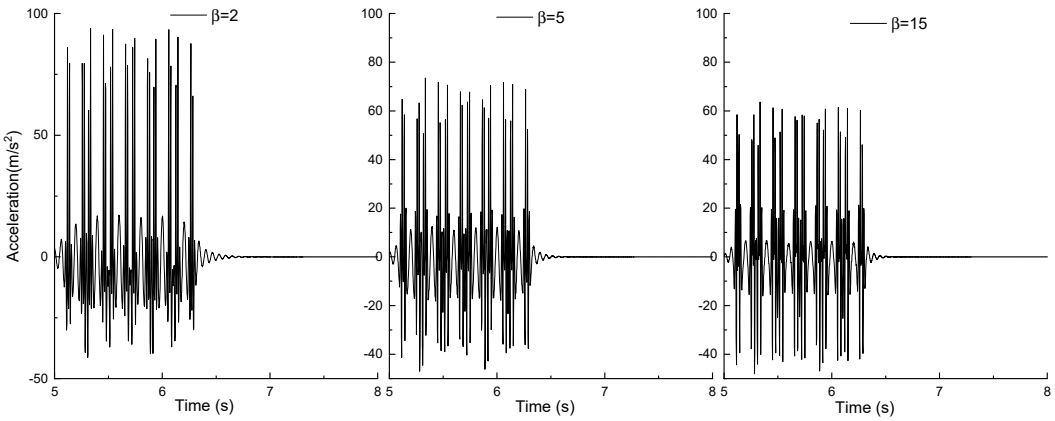

Figure 11. Time history curve of ground acceleration at the track center at 130 m/s.

When the train load acts on the track, it generates reciprocating downward and upward acceleration as the wheel set passes by. The downward acceleration has a compaction effect on the foundation soil, and does not cause damage to the foundation as long as it is below the acceleration corresponding to the critical compressive strength of the soil. Meanwhile, the upward acceleration generates tensile stress in the foundation, which may exceed the fragile tensile strength of the soil, and this cyclic effect will inevitably have a certain impact on the structural integrity and operational stability of the foundation soil and nearby infrastructure. From Figures 9–11, it can be seen that at low speed, cross speed, and high speed, when the soil homogeneity coefficient increases from 2 to 5 and then to 15, the downward acceleration magnitude gradually decreases, and the reduction percentage of the upward acceleration amplitude is about 9%, 25%, and 33%, respectively. Therefore, it can be inferred that increasing the homogeneity coefficient is beneficial for the maintenance of the foundation, especially at cross and high speeds.

The ground vertical displacement at the track center will affect the safety and comfort of HSR. Figures 12–14 shows the time history curve of ground vertical displacement at the track center at different homogeneity coefficients, and the train speeds are 60 m/s, 94.5 m/s, and 130 m/s respectively. The ground displacement also exhibits a quasi-static effect of the wheel axle at 60 m/s and 94.5 m/s, and we can clearly see the footprints of the train wheels acting on the track. At the high speed of 130 m/s, the ground vibration acceleration displays a fluctuating effect, which may be caused by the resonance of the track–ground system when the train speed is high, up to a certain value. It can be seen from Figures 12–14 that, contrary to the ground acceleration situation, the downward ground displacement is much larger than that of the upward displacement. The downward displacement decreases as β increases from 2 to 5; however, the peak displacement change is not significant as β increases from 5 to 15. At the high speed of 130 m/s, the ground acceleration shows a more obvious fluctuating effect at β = 2, which means weaker homogeneity of the ground soil. Improving soil homogeneity is beneficial for mitigating the ground displacement at the track center; however, the impact is limited as the value of β exceeds 5. From Figures 12–14, it can also be seen that at low speed, cross speed, and high speed, when the soil homogeneity coefficient increases from 2 to 15, the downward displacement magnitude decreases, and the reduction percentage of the displacement amplitude is about 22.2%, 34.4%, and 38.5%, respectively. Combining the analysis of Figures 9–11, it can be concluded that, as the train speed increases from low speed to high speed, increasing the value of β can significantly reduce the ground vibration characteristics at the track center.

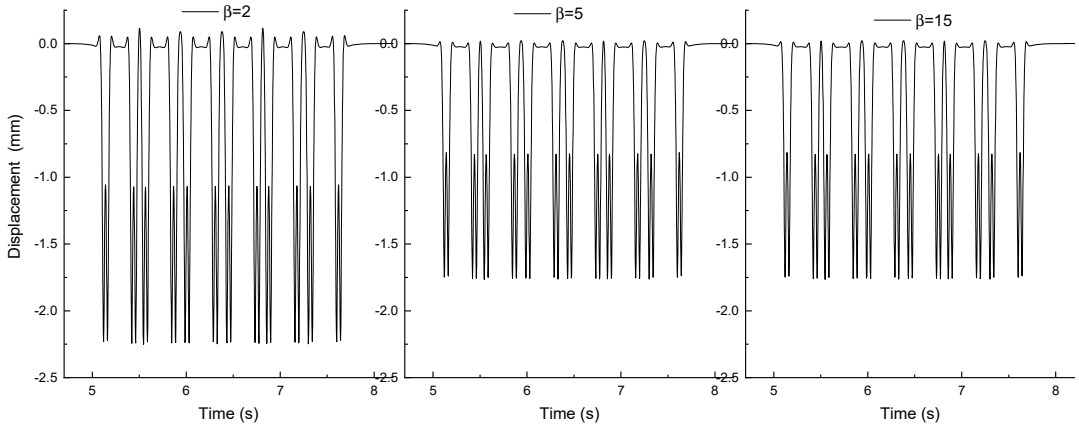

Figure 12. Time history curve of ground displacement at the track center at 60 m/s.

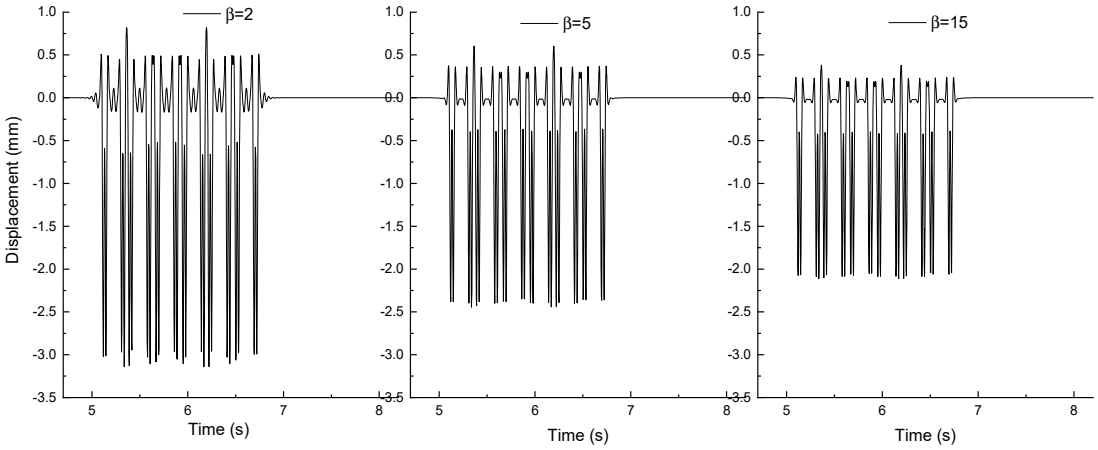

Figure 13. Time history curve of ground displacement at the track center at 94.5 m/s.

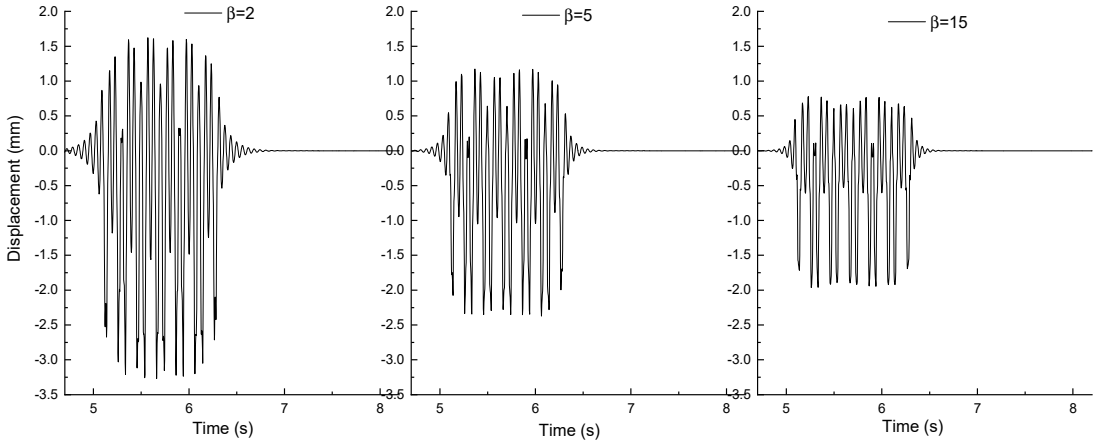

Figure 14. Time history curve of ground displacement at the track center at 130 m/s.

To study the law of variation of ground vibration with train speed and soil uniformity, a numerical simulation is conducted to obtain the ground vibration velocity, displacement, and acceleration under different speeds and uniformity coefficients. Figure 15 shows the ground vibration amplitude attenuation with the distance from the track center at different soil homogeneity coefficients and train speeds. It can be found that, in low-speed, cross-speed, and high-speed conditions, the vibration amplitude near the track center increases significantly as coefficient β decreases from 15 to 2. At a lower speed of 60 m/s, the spatial influencing range of the homogeneity coefficient on the vibration amplitude is about 0–2 m. At a cross speed of 94.5 m/s, the influencing range is 0–8 m. As the speed further increases to a higher speed of 130 m/s, the influencing range increases to 0–10 m. That is to say, at cross speed and high speed, the β influencing range increases to 0–10 m from 0–2 m at a speed of 60 m/s, and the apparent fluctuation effect in the far distance can be observed. In the cross-speed condition, a phenomenon of an increase in the local rebound of the velocity and acceleration attenuation curve can be observed as the coefficient β decreases to 2, which is consistent with the data and findings in previous research [41–44]. This may be caused by defects in the soil area, with a very low elastic modulus in the non-uniform superficial soil, which has an increased dynamic response at some certain resonance train speed. Therefore, it can be inferred that, an obvious Doppler effect and vibration amplification zones may occur in the ground vibration in cross-speed or high-speed conditions, and the lateral fluctuation range and vertical vibration intensity increase significantly, especially in non-improved soil with low homogeneity. This indicates that in practical engineering, when the speed is low, the influence of surface soil uniformity on the prediction of the ground vibration amplitude near the track should not be ignored; when the speed increases

above the cross speed, the influence of surface soil uniformity on the prediction of the ground vibration amplitude far from the track should also be considered. In high-speed conditions, the maximum acceleration does not occur at the track center but at a distance about 1 m away from the center, which is also illustrated by the work of some previous studies [12]; the maximum acceleration appears near the outer edges of the composite track beam under the dynamic action of higher speed loads.

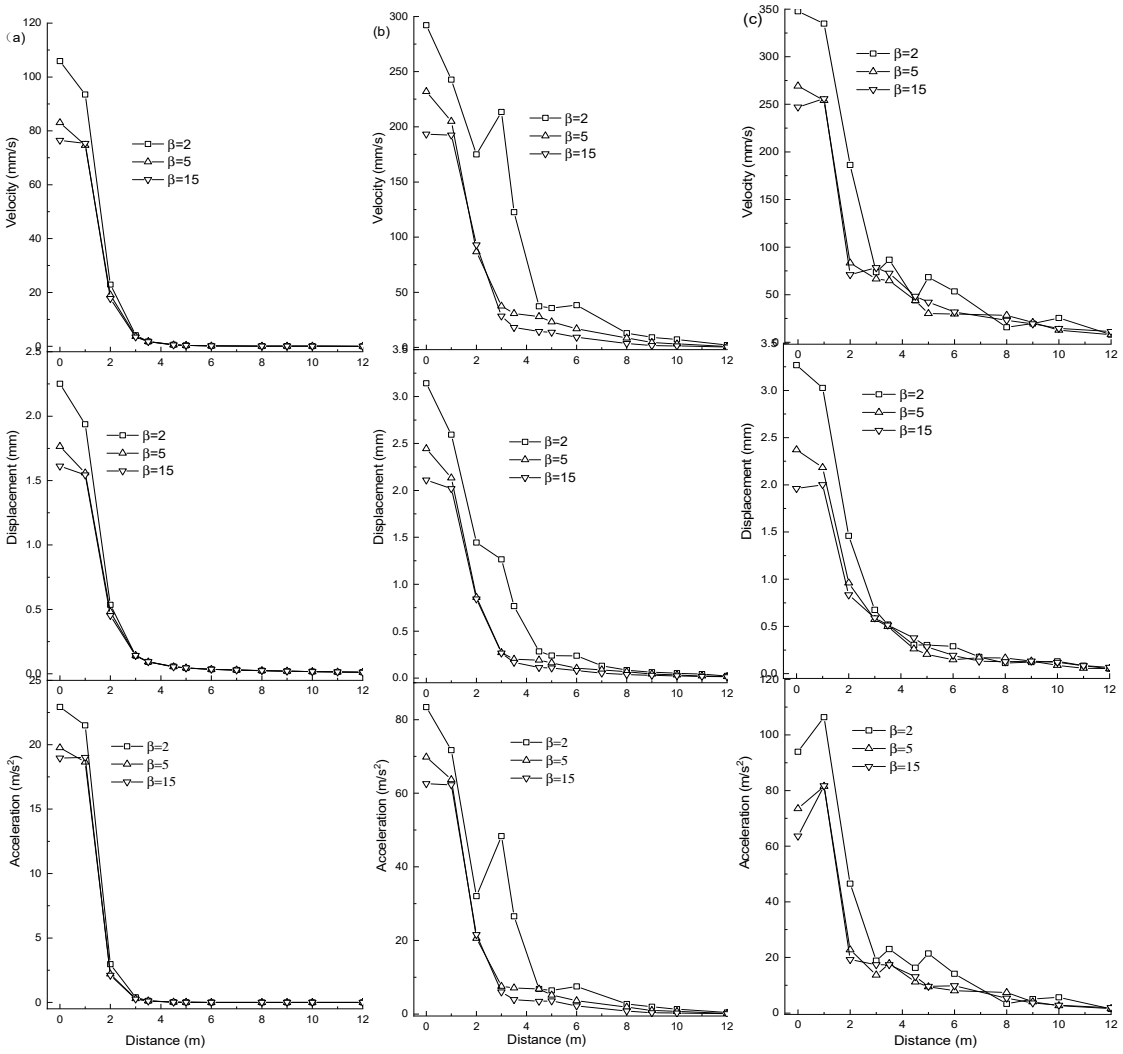

Figure 15. Ground vibration attenuation at different values β and speed: (**a**) 60 m/s; (**b**) 94.5 m/s; (**c**) 130 m/s.

5. Conclusions and Further Discussion

This paper presents a high-efficiency numerical method to solve the coupled track–ground system. The calculation procedure for analyzing the non-uniform ground vibration caused by a high-speed train is proposed, and the track-non-uniform layered ground model is established based on the elastic 2.5D FEM and the theory of stochastic variables. The propagation and attenuation of non-uniform layered ground vibration at different train speeds are investigated. The following conclusions can be drawn:

(1) The variation in the soil elastic modulus and train speed has the most important influence on ground vibration; at low speed, the soil homogeneity coefficient has almost no influence on the shape of the acceleration time history curve.

(2) The acceleration upward is much larger than the acceleration downward at most speeds; at cross speed and high speed, the acceleration amplitude decreases with the increase in the homogeneity coefficient.

(3) At low speed and cross speed, both upward and downward peak acceleration at the track center decrease significantly as the homogeneity coefficient increases from 2 to 5; at high speed, the upward peak acceleration continues to decrease as the homogeneity coefficient increases from 2 to 15, while the downward peak value increases slightly.
(4) At cross speed and high speed, an apparent fluctuation effect can be observed at a far distance, and the influencing range of the homogeneity coefficient increases to 0–10 m from 0–2 m as the train speed increases from 60 m/s to 130 m/s.
(5) At cross speed, a phenomenon of an increase in the local rebound in the velocity and acceleration attenuation curve can be observed as the homogeneity coefficient decreases to 2, and the maximum acceleration occurs near the outer edge of the composite track as the ground soil has weaker homogeneity.

The proposed high-efficiency 2.5D random FEM in this article has promising application prospects. It can be applied not only to the analysis of the ground vibration in sensitive environments caused by high-speed rail operation, but also to other application scenarios involving moving loads, such as heavy-haul railway, large freight cars, underground subways, and aircraft loads, with consideration of the ground non-homogeneity. It can also be used to study the response of linear project structures (such as tunnels, long bridges, or pipeline) to traveling seismic waves. In addition, if the obtained vibration displacement is used for further finite element calculation, the vibration stress and strain data of the foundation near the load can also be obtained, based on which the ground strength damage and cumulative deformation can be analyzed. This is of great significance for the operation assessment and maintenance of foundation facilities. Hence, compared to traditional 3D finite element methods, the proposed method in this article is a promising tool worthy of further exploration.

Nonetheless, in the traditional 3D finite element calculation, there may be some shortcomings, including volumetric locking and poor accuracy when simple triangular elements are used. In recent years, authors have been dedicated to researching methods for improving the efficiency in the finite element method [15,42–46]. By applying Fourier transform in the train's moving direction and using the four-node isoparametric elements, the proposed 2.5D finite element method can avoid the volumetric locking problems and improve the computational efficiency with high accuracy. However, besides the FEM, it is undeniable that some other numerical methods have been developed which have their own advantages, for example, mesh-free methods including the smoothed point interpolation method (SPIM), material point method (MPM), and smooth particle hydrodynamics (SPH) [47–49]. In our study dealing with the dynamic response of a roadbed under random roughness conditions, the 2.5D FEM requires repeated calculation at each harmonic component of the roughness spectrum, which will no longer highlight the advantage of the high efficiency of 2.5D FEM. Taking advantage of the other methods [47–49] in future research may improve the proposed method for better study of the non-uniform ground response under moving loads with track roughness conditions.

Moreover, as mentioned in this article, although the introduction of the random variable model in the 2.5D FEM makes it possible to take into account soil non-uniformity, the heterogeneity of the soil is quite a complex issue which is difficult to accurately describe. The Weibull statistical distribution in the present paper provides a perspective for the consideration of soil spatial variability. In further study, the normal distribution, stochastic field theory, or distribution models obtained through back-analysis based on in situ testing may be used to improve the description of the heterogeneity characteristics of the ground soil.

Author Contributions: Conceptualization, S.Y. and W.X.; methodology, S.Y. and W.X.; validation, S.Z., W.W. and L.Y.; formal analysis, S.T., S.Z., J.L., W.W. and S.Y.; writing—original draft preparation, visualization, S.Y.; writing—review and editing, S.Z.; project administration, W.W.; funding acquisition, W.W. All authors have read and agreed to the published version of the manuscript.

Funding: The project was financial supported by the National Natural Science Foundation of China (Grant No. 42277130), which is gratefully acknowledged.

Data Availability Statement: Data available upon request.

Conflicts of Interest: Author Wei Xie was employed by the company Powerchina Huadong Engineering Co., Ltd. Authors Shuo Tang and Jinglong Liu were employed by the company Tianjin Branch, CNOOC (China) Co., Ltd. The remaining authors declare that the research was conducted in the absence of any commercial or financial relationships that could be construed as a potential conflict of interest.

References

1. Xia, H. *Traffic Environment Vibration Engineering*; Science Press: Beijing, China, 2010.
2. Beskou, N.D.; Theodorakopoulos, D.D. Dynamic effects of moving loads on road pavements: A review. *Soil Dyn. Earthq. Eng.* **2011**, *31*, 547–567. [CrossRef]
3. Eason, G. The stresses produced in a semi-infinite solid by a moving surface force. *Int. J. Eng. Sci.* **1965**, *2*, 581–609. [CrossRef]
4. Lu, Z.; Hu, Z.; Yao, H.; Liu, J.; Zhan, Y. An analytical method for evaluating highway embankment responses with consideration of dynamic wheel–pavement interactions. *Soil Dyn. Earthq. Eng.* **2016**, *83*, 135–147. [CrossRef]
5. Fiala, P.; Degrande, G.; Augusztinovicz, F. Numerical modelling of ground-borne noise and vibration in buildings due to surface rail traffic. *J. Sound Vib.* **2007**, *301*, 718–738. [CrossRef]
6. Lefeuve-Mesgouez, G.; Mesgouez, A. Three-dimensional dynamic response of a porous multilayered ground under moving loads of various distributions. *Adv. Eng. Softw.* **2012**, *46*, 75–84. [CrossRef]
7. Dieterman, H.A.; Metrikine, A. Steady-state displacements of a beam on an elastic half-space due to a uniformly moving constant load. *Eur. J. Mech. A/Solids* **1997**, *16*, 295–306.
8. Sheng, X.; Jones, C.; Petyt, M. Ground vibration generated by a load moving along a railway track. *J. Sound Vib.* **1999**, *228*, 129–156. [CrossRef]
9. Yang, Y.; Hung, H. A 2.5D finite/infinite element approach for modelling visco-elastic bodies subjected to moving loads. *Int. J. Numer. Methods Eng.* **2001**, *51*, 1317–1336. [CrossRef]
10. Yang, Y.B.; Hung, H.H.; Chang, D.W. Train-induced wave propagation in multi-layered soils using finite/infinite element simulation. *Soil Dyn. Earthq. Eng.* **2003**, *23*, 263–278. [CrossRef]
11. Takemiya, H.; Bian, X. Substructure simulation of inhomogeneous track and layered ground dynamic interaction under train passage. *J. Eng. Mech.* **2005**, *131*, 699–711. [CrossRef]
12. Bian, X.; Chen, Y.; Hu, T. Numerical simulation of high-speed train induced ground vibrations using 2.5D finite element approach. *Sci. China Ser. G Phys. Mech. Astron.* **2008**, *51*, 632–650. [CrossRef]
13. Bian, X.; Jiang, H.; Chang, C.; Hu, J.; Chen, Y. Track and ground vibrations generated by high-speed train running on ballastless railway with excitation of vertical track irregularities. *Soil Dyn. Earthq. Eng.* **2015**, *76*, 29–43. [CrossRef]
14. Gao, G.; Chen, Q.; He, J.; Liu, F. Investigation of ground vibration due to trains moving on saturated multi-layered ground by 2.5D finite element method. *Soil Dyn. Earthq. Eng.* **2012**, *40*, 87–98. [CrossRef]
15. Gao, G.; Yao, S.; Yang, J.; Chen, J. Investigating ground vibration induced by moving train loads on unsaturated ground using 2.5D FEM. *Soil Dyn. Earthq. Eng.* **2019**, *124*, 72–85. [CrossRef]
16. Sheng, X.; Jones, C.J.C.; Thompson, D.J. A theoretical study on the influence of the track on train-induced ground vibration. *J. Sound Vib.* **2004**, *272*, 909–936. [CrossRef]
17. Phoon, K.K.; Kulhawy, F.H. Evaluation of geotechnical property variability. *Can. Geotech. J.* **1999**, *36*, 625–639. [CrossRef]
18. Wang, M.X.; Wu, Q.; Li, D.Q.; Du, W. Numerical-based seismic displacement hazard analysis for earth slopes considering spatially variable soils. *Soil Dyn. Earthq. Eng.* **2023**, *171*, 107967. [CrossRef]
19. Auersch, L. Ground vibration due to railway traffic—The calculation of the effects of moving static loads and their experimental verification. *J. Sound Vib.* **2006**, *293*, 599–610. [CrossRef]
20. Hu, H.; Huang, Y. PDEM-based stochastic seismic response analysis of sites with spatially variable soil properties. *Soil Dyn. Earthq. Eng.* **2019**, *125*, 105736. [CrossRef]
21. Deng, E.; Liu, X.Y.; Ni, Y.Q.; Wang, Y.W.; Zhao, C.Y. A coupling analysis method of foundation soil dynamic responses induced by metro train based on PDEM and stochastic field theory. *Comput. Geotech.* **2023**, *154*, 105180. [CrossRef]
22. Wang, Y.; He, J.; Shu, S.; Zhang, H.; Wu, Y. Seismic responses of rectangular tunnels in liquefiable soil considering spatial variability of soil properties. *Soil Dyn. Earthq. Eng.* **2022**, *162*, 107489. [CrossRef]
23. Papadopoulos, M.; François, S.; Degrande, G.; Lombaert, G. The influence of uncertain local subsoil conditions on the response of buildings to ground vibration. *J. Sound Vib.* **2018**, *418*, 200–220. [CrossRef]
24. Alamanis, N.; Dakoulas, P. Effects of spatial variability of soil properties and ground motion characteristics on permanent dis-placements of slopes. *Soil Dyn. Earthq. Eng.* **2022**, *161*, 1–22. [CrossRef]
25. Zhang, L.L. *Reliability Theory of Geotechnical Engineering*; Tongji University Press: Shanghai, China, 2011.
26. Coelho, B.Z.; Nuttall, J.; Noordam, A.; Dijkstra, J. The impact of soil variability on uncertainty in predictions of induced vibrations. *Soil Dyn. Earthq. Eng.* **2023**, *169*. [CrossRef]

27. Kouroussis, G.; Vogiatzis, K.E.; Connolly, D.P. A combined numerical/experimental prediction method for urban railway vibration. *Soil Dyn. Earthq. Eng.* **2017**, *97*, 377–386. [CrossRef]
28. dos Santos, N.C.; Barbosa, J.; Calçada, R.; Delgado, R. Track-ground vibrations induced by railway traffic: Experimental validation of a 3D numerical model. *Soil Dyn. Earthq. Eng.* **2017**, *97*, 324–344. [CrossRef]
29. Connolly, D.; Galvín, P.; Olivier, B.; Romero, A.; Kouroussis, G. A 2.5D time-frequency domain model for railway induced soil-building vibration due to railway defects. *Soil Dyn. Earthq. Eng.* **2019**, *12*, 332–344. [CrossRef]
30. Gao, G.Y.; Chen, G.Q.; Zhang, B. Analysis of active isolation of vertical non uniform fundamental wave barrier under train load. *Vib. Shock.* **2013**, *32*, 57–62. (In Chinese)
31. Zhou, F.; Cao, Y.; Zhao, W. Dynamic response analysis of non-uniform foundation under moving loads. *Geotech. Mech.* **2015**, *36*, 2027–2033. (In Chinese)
32. Ma, Q.; Zhou, F. Dynamic response of gradient non-uniform soil under moving loads. *J. Nat. Disasters* **2018**, *27*, 61–67.
33. Bert, C.W.; Moinuddin, M. Differential quadrature: A powerful new technique for analysis of composite structures. *Compos. Struct.* **1997**, *39*, 179–189. [CrossRef]
34. Wang, Y.; Gu, Y.; Liu, J. A domain-decomposition generalized finite difference method for stress analysis in three-dimensional composite materials. *Appl. Math. Lett.* **2020**, *104*, 106226. [CrossRef]
35. Meng, Z.; Wang, Y.; Zheng, S.; Wang, X.; Liu, D.; Zhang, J.; Shao, Y. Abnormal monitoring data detection based on matrix manipulation and the cuckoo search algorithm. *Mathematics* **2024**, *12*, 1345. [CrossRef]
36. Tang, C.A.; Liu, H.; Lee, P.K.K. Numerical studies of the influence of microstructure on rock failure in uniaxial compression-Part I: Effect of heterogeneity. *Int. J. Rock Mech. Min. Sci.* **2000**, *37*, 555–569. [CrossRef]
37. Jinsheng, L.; Zenglin, W.; Qi, Y. Rand model of heterogeneous formation physical parameters based on Weibull distribution. *J. Undergr. Space Eng.* **2017**, *13*, 115–122.
38. Liu, J.B.; Li, B. A unified viscous-spring artificial boundary for 3-D static and dynamic applications. *Sci. China (Ser. E)* **2005**, *35*, 570–584. [CrossRef]
39. Costa, P.A.; Colaço, A.; Calçada, R.; Cardoso, A.S. Critical speed of railway tracks. Detailed and simplified approaches. *Transp. Geotech.* **2015**, *2*, 30–46. [CrossRef]
40. Zhai, W.M.; Han, H.Y. Research on ground vibration caused by high-speed trains running on soft soil foundation lines. *Sci. China (Ser. E)* **2012**, *42*, 1148–1156.
41. Liang, R.; Liu, W.; Ma, M.; Liu, W. An efficient model for predicting the train-induced ground-borne vibration and uncertainty quantification based on Bayesian neural network. *J. Sound Vib.* **2020**, *495*, 908–922. [CrossRef]
42. Gao, G.Y.; Yao, S.F.; Sun, Y.M. Unsaturated ground vibration induced by high-speed train loads based on 2.5D finite element method. *J. Tongji Univ.* **2019**, *47*, 957–966. (In Chinese)
43. Gao, G.Y.; Yao, S.F.; Yang, C.B. Ground vibration induced by moving train loads on unsaturated soil using 2.5D FEM. *J. Harbin Inst. Technol.* **2019**, *51*, 95–103. (In Chinese)
44. Gao, G.Y.; Yao, S.F.; Sun, Y.M. 2.5D Finite Element analysis of unsaturated ground vibration induced by High Speed Rail Load. *Earth-Quake Eng. Eng. Vib.* **2019**, *33*, 234–245.
45. Gao, G.; Yao, S.; Cui, Y.; Chen, Q.; Zhang, X.; Wang, K. Zoning of confined aquifers inrush and quicksand in Shanghai region. *Nat. Hazards* **2018**, *91*, 1341–1363. [CrossRef]
46. Dell, F.; Di Tommaso, F.; Guessab, A.; Nudo, F. A general class of enriched methods for the simplicial linear finite elements. *Appl. Math. Comput.* **2023**, *456*, 128149.
47. Bandara, S.; Soga, K. Coupling of soil deformation and pore fluid flow using material point method. *Comput. Geotech.* **2015**, *63*, 199–214. [CrossRef]
48. Dezfooli, M.S.; Khoshghalb, A.; Shafee, A. An automatic adaptive edge-based smoothed point interpolation method for coupled flow-deformation analysis of saturated porous media. *Comput. Geotech.* **2022**, *145*, 104672. [CrossRef]
49. Bui, H.H.; Fukagawa, R.; Sako, K.; Ohno, S. Lagrangian meshfree particles method (SPH) for large deformation and failure flows of geomaterial using elastic–plastic soil constitutive model. *Int. J. Numer. Anal. Methods Géoméch.* **2008**, *32*, 1537–1570. [CrossRef]